UPSCALING OF PEROVSKITE-SILICON TANDEM SOLAR CELLS

O. Schultz-Wittmann[1], P. S. C. Schulze[1], O. Er-Raji[1,3], R. Efinger[1], Ö. Ş. Kabaklı[1], M. Heydarian[1,3], K. A. McMullin[1], O. Fischer[1,3], A. J. Bett[1], D. Erath[1], S. Pingel[1], U. Heitmann[1], Z. Kiaee[1], M. Kohlstädt[1], B. P. Kore[1,3], H. Nagel[1], M. C. Schubert[1], M. Bivour[1], J. C. Goldschmidt[1,2], J. Borchert[1,3], M. Hermle[1], S. W. Glunz[1,3]
[1] Fraunhofer Institute for Solar Energy System (ISE), Heidenhofstr. 2, 79110 Freiburg, Germany
Email: oliver.schultz-wittmann@ise.fraunhofer.de,
[2] Philipps-University Marburg, Renthof 7, 35032 Marburg, Germany
[3]INATECH, University of Freiburg, Emmy-Noether Str.2, 79110 Freiburg, Germany

ABSTRACT: We are working on upscaling of perovskite-silicon tandem solar cells from small lab size areas of several square millimeters to full commercial wafer size. This requires the use of processing techniques that can replace the usual spin coating process employed for small lab size areas. As alternatives for large-area depositions spray coating, inkjet printing and slot-die coating are investigated. For highest specific energy yield under field conditions perovskite-silicon tandem solar cells should be textured on the front side. To ensure conformal coating of the random pyramid textured silicon bottom cell we follow a hybrid process route. In a first step, the inorganic components are thermally evaporated to form a scaffold allowing conformal coating of pyramids of arbitrary size and shape. In a second step, the conversion into perovskite is accomplished by infiltration of the scaffold with organic salt solutions. A thermal anneal completes the conversion into a polycrystalline perovskite layer.
In addition to upscaling of the cell area we work on replacing the evaporated silver contact grid by screen printed ultra-low temperature silver paste. First results on planar perovskite-silicon tandem solar cells, still fabricated with spin coating processing but with screen-printed front contacts, resulted in a certified stabilized conversion efficiency of 22.5% on 104 cm^2 total cell area.
Keywords: Perovskites, Tandem, Hybrid

1 INTRODUCTION

Perovskite-silicon tandem solar cells with highest specific energy yield under field conditions should be textured on the front side [1]. Since the standard lab procedures of wet-chemical processing like spin-, spray- or blade coating do not yield conformal coating of µm-sized textured surfaces, we follow a hybrid route to deposit mixed cation mixed halide perovskite absorbers $[HC(NH_2)_2]_{1-x}Cs_xPb(I_{1-y}Br_y)_3$ [2,3]. In a first step, the inorganic components are thermally evaporated to form a scaffold allowing conformal coating of pyramids of arbitrary size and shape. In a second step, the conversion into perovskite is accomplished by infiltration with organic salt solutions. For the second step, several deposition techniques are evaluated which are already used in other industrial fields: a) spray coating b) inkjet printing c) slot-die coating (Figure 1). An annealing process finalizes formation of a polycrystalline perovskite.

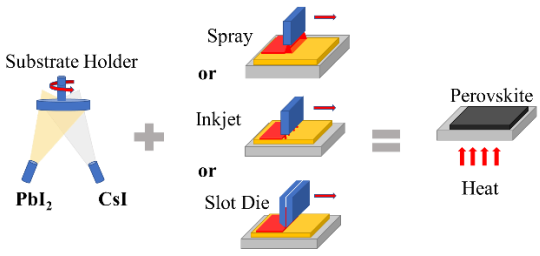

Figure 1: Illustration of hybrid route used for perovskite deposition onto µm-sized textured substrates. We evaporate a porous PbI_2/CsI scaffold (yellow) onto a silicon bottom cell and infiltrate this layer with an organic salt solution (red). After an annealing process a polycrystalline perovskite (black) is formed.

Sintering of screen-printed silver paste in a high-temperature firing process is the standard industrial process for metallization of single-junction silicon solar cells. However, perovskites are temperature-sensitive, hence for this approach ultra-low temperature pastes that cure below 150°C are required [4] and will be used in our experiments.

On medium size solar cells of 4 cm^2 full area, we analyze the impact of shunts that are distributed across the entire cell area. Such shunts are often not present in small area (1 cm^2) champion cells because of the ability to select small shunt-free cells for analysis.

2 EXPERIMENTAL

2.1 Tandem Cell Structure

As silicon bottom cells we used 250 µm thick boron-doped Float Zone wafers of 1 Ω cm resistivity and amorphous silicon heterojunction surfaces [5]. The rear electrode consists of evaporated silver whereas on the front side a ca. 20 nm thick ITO completes the bottom cell preparation. The top cells were prepared by spin coating of hole transport layers (HTL) followed by spin coating of perovskite solution for the case of planar front or by co-evaporation of PbI_2/CsI for textured surfaces. For this hybrid route subsequent infiltration of the inorganic scaffold was accomplished by either spin coating of organic salt solutions as our reference process or by spray coating or inkjet printing as our target process sequence. Subsequently, a thin layer of C_{60} was evaporated followed by atomic layer deposition of SnO_x and sputtering of ITO. The front electrode was either prepared by evaporation of silver through a shadow mask or screen-printing of an ultra-low temperature silver paste. Finally, a MgF_2 anti reflection layer was evaporated on top (Figure 2).

We used two different approaches for the deposition of the perovskite layers: For planar front sides established spin coating processing was used while for textured surfaces we used a hybrid approach. For cell areas of 5x5 mm^2, 10x10 mm^2 and 20x20 mm^2 we used evaporated silver through a shadow mask as the method for front metallization. For even larger areas of 50x50 mm^2 and 102x102 mm^2 we used screen printing of silver paste, that can cure at very low temperatures of about 130 °C.

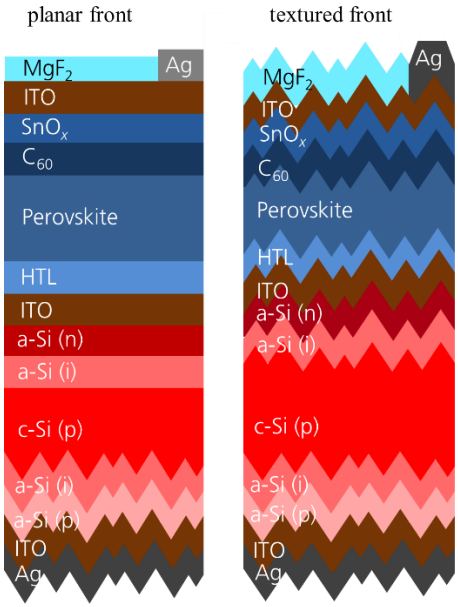

Figure 2: Perovskite-silicon tandem solar cell structure with planar or textured front.

2.2 Characterization

After certain processing steps we used photo-luminescence imaging to assess the material quality and homogeneity of the prepared layers [6]. Using blue generation light of 450 nm allowed to selectively excite the perovskite cell. Also, we used lock-in thermography [6,7] to identify shunted areas.

For *IV* measurements the definition of the active cell area is of major importance. The layout for the different solar cell structures is shown in Figure 3 where the small cell design consists of four 5x5 mm^2 area with a U-shape metallization on a 25x25mm^2 substrate. In such a design the *IV* measurements are made on the "designated area" (d.a.) which is not metallized [8]. For 10x10 mm^2 and 20x20 mm^2 cells the metallization fingers are part of the active cell area but the broad circumferent metallization busbar is not considered part of the active area, again resulting in a "designated area" measurement. For large-area cells we have cut out the cell boundaries by laser scribing and cleaving. Hence, the entire remaining wafer, including the metallization grid, is considered being part of the active area and the IV measurement is described as a "total area" (t.a.) measurement.

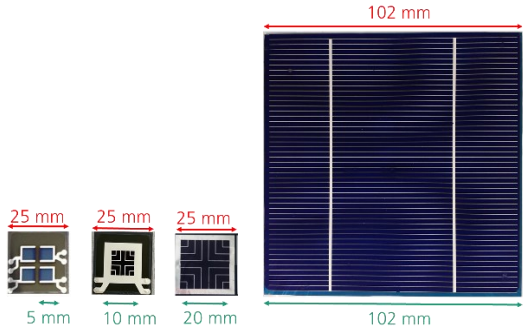

Figure 3: Tandem cell layout and area definitions for *IV* measurements. Red: Substrate dimension. Green: Active cell dimension.

3 RESULTS AND DISCUSSION

3.1 Spin Coating of Perovskite Absorber

When scaling up the area of perovskite-silicon tandem cells homogeneity of layer quality as well as density and severity of shunts are key performance indicators. In the following experiments processing of the perovskite was performed with spin coating, which is the established lab process for small areas. However, we also used it for larger areas to test the limit for this approach. We have observed that with adjustment of the processing parameters (spin speed, volume of liquid etc.) reasonably homogeneous layer properties could be obtained in the center of 100 mm diameter wafers. This can be concluded from Figure 4 where a photoluminescence image irradiated with 450 nm wavelength with an intensity of about 587 Wm^{-2} is shown for a wafer with 100 mm diameter containing seven individual cells of 20x20 mm^2 active area. The corresponding *IV* measurements reveal similarly small spread of power conversion efficiency.

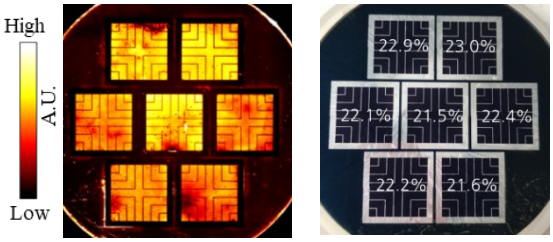

Figure 4: 7 perovskite-silicon tandem solar cells of 20x20 mm^2 active area on a 100 mm diameter wafer. Left: Photoluminescence image excited with 450 nm light. Right: Picture of the same wafer with corresponding power conversion efficiencies averaged from IV measurements in forward and reverse direction.

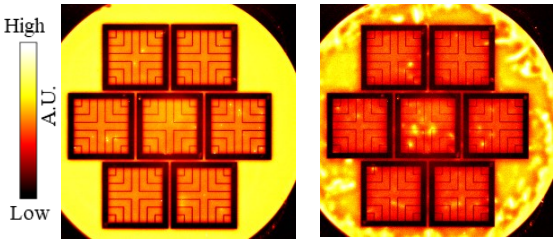

Figure 5 Left: Illuminated Lock-In Thermography (ILIT) image of the perovskite sub cells using a blue 470 nm LED for the excitation of charge carriers. Right: ILIT image of the silicon sub cells using an infrared 950 nm LED for excitation. Bright spots within the active area of the solar cells mark regions with increased heat dissipation. Consequently, in these regions ohmic shunts or increased non-radiative recombination can be found.

In Figure 5 a measurement of the same wafer with Illuminated Lock-In Thermography (ILIT) is shown. The use of blue light for excitation of charge carriers allows measurement of the top cell. Likewise, infrared light is used to measure the silicon bottom cell. Bright spots within the active area reveal locations of increased heat dissipation, hence one can find ohmic shunts (or increased non-radiative recombination) in those locations. While these spots are frequently found in the perovskite top cell, they are also found in the silicon bottom cell. This stresses the need to have high quality for both sub cells that combined work as a tandem cell.

We made further attempts to increase the area on planar cells with spin coating of the perovskite absorber. The PL imaging results for a large cell of 102x102 mm^2 perovskite-silicon tandem cell can be seen in Figure 6a. Excitation with 450 nm wavelength allows for selectively detecting the signal of the top cell and strong inhomogeneities are revealed. This indicates that such large area is beyond the current process maturity of the spin coating process for the perovskite absorber. Hence, we tested the hybrid route for the case of inkjet printing (Figure 6b) and spray coating (Figure 6c). Though for the inkjet printed sample 3 mm wide stripes are observed, overall homogeneity is greatly improved. Also, these stripes can be avoided by a set-up in which the entire area will be printed in a single swath rather than in multiple passes covering 3 mm on each pass. Similarly, the spray coating sample also exhibits a much more homogeneous PL signal. A small gradient from top to bottom is observed but these results support the confidence into the hybrid route approach for large-area perovskite-silicon tandem solar cells.

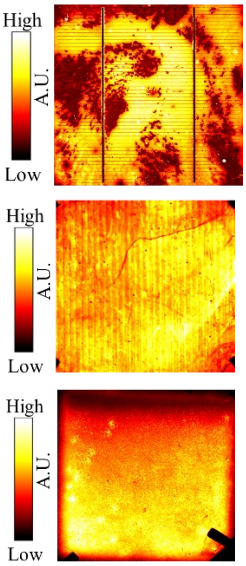

a) 102x102 mm^2 tandem cell prepared by spin coating. The resulting top cell shows a strongly inhomogeneous PL signal.

b) 100x100 mm^2 top cell prepared by hybrid route with inkjet printing. While stripes are visible overall homogeneity is improved.

c) 100x100 mm^2 top cell prepared by hybrid route with spray coating. While a gradient is observed overall homogeneity is improved.

Figure 6: PL images of perovskite layers on planar surfaces excited by a 450 nm laser.

3.2 Hybrid Route

In order to obtain a conformal coating of the surface also for textured bottom cells we follow the hybrid route. In a first step, the inorganic components are thermally evaporated to form a scaffold allowing conformal coating of pyramids of arbitrary size and shape. A cross section SEM image is shown in Figure 7 (top). In a second step, the conversion into perovskite is accomplished by infiltration of the porous scaffold with organic salt solutions.

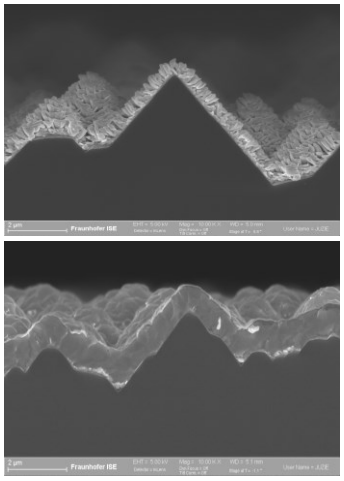

Figure 7: SEM images of evaporated PbI_2/CsI scaffold (top image) and after infiltration with organic salt solution and crystallization (bottom image).

In the SEM image in Figure 7 (bottom) this was accomplished by spin coating but inkjet printing and spray coating yield the same results and a conformal coating of the textured surface is obtained. This texture on the front side is intended to not only increase the power conversion efficiency of the cell but also the performance ratio over the year in a fixed tilt installation [1]. The change in the relative EQE shape for a textured cell produced by the hybrid route and a planar cell is shown in Figure 8. Compared to the planar front the EQE becomes flatter.

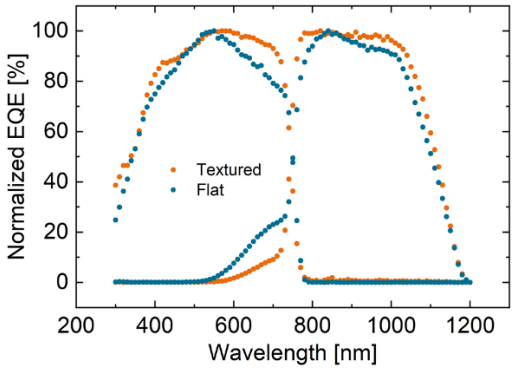

Figure 8: Relative EQE measurements of a textured and a planar perovskite-silicon tandem cell normalized to 100% on the respective highest measurement data points. The change in the shape of the EQE is related to the front texture.

3.3 *IV* Results

In Table 1 *IV* results of perovskite-silicon tandem solar cells made at Fraunhofer ISE are shown. The upper rows show measurements in forward direction, the lower rows in reverse and η_{steady} is the stabilized steady state efficiency value.

Cell A is textured and was produced with the hybrid route where the infiltration of the inorganic scaffold was accomplished by spin coating of organic salts. Cells B and C have a planar front and the perovskite was produced by spin coating. With a total area of 104 cm^2 cell C is the largest cell we have produced so far and has a screen-printed silver metallization of the front.

Table 1 : *IV*-parameters of recent perovskite-silicon tandem solar cells of varying size made at Fraunhofer ISE. The upper rows show measurement in forward direction, the lower rows in reverse.
*Calibrated measurement at Fraunhofer ISE CalLab
A: textured front, hybrid route, evaporated metal
B: planar front, evaporated metal
C: planar front, screen-printed metal

#	*Area* [cm^2]	η_{steady} [%]	j_{sc} [mA cm^{-2}]	V_{oc} [mV]	*FF* [%]	η [%]
A	$1.0_{d.a.}$	25.2	18.0	1786	77.4	24.9
			18.1	1786	77.6	25.0
B	$4.0_{d.a}$	23.0*	17.0	1771	75.1	22.7
			17.0	1771	75.1	22.6
C	$104_{t.a}$	22.5*	17.8	1772	68.2	21.5
			17.9	1771	70.5	22.4

4 SUMMARY AND CONCLUSIONS

We fabricated textured perovskite-silicon tandem solar cells with a hybrid processing route. This resulted in the formation of a top solar cell that conformally coats the µm-sized random pyramid texture of the bottom solar cell. Initial results on 1 cm^2 designated area reached 25.2% where the infiltration of the inorganic scaffold was accomplished by spin coating of organic salts.

Increasing the area on planar surfaces using spin coating for the perovskite formation was successful and for very large cells of 104 cm^2 total area we reached certified 22.5% stabilized steady state efficiency. Furthermore, we managed to integrate screen-printing of a low-temperature silver paste curing at 130 °C for the front metallization. However, inhomogeneities in the top cell have been detected by photoluminescence as the area increased. Hence, we work on replacement of the spin coating process. Inkjet printing as well as spray coating show promising initial results on large areas.

As a next step we will replace the spin coating process in the hybrid route by inkjet printing or spray coating. We expect this to enable cell efficiencies in the range of 28% for large area, textured perovskite silicon tandem cells with printed metallization.

5 ACKNOWLEDGEMENTS

This work was partially funded by the German Federal Ministry for Economics Affairs and Climate Action under contract number 03EE1086A (PrEsto) and 03EE1087A (Katana) as well as a Fraunhofer LIGHTHOUSE PROJECT (MaNiTU). Ö. Ş. Kabaklı gratefully acknowledges scholarship from the Dr. Ruth Heerdt Stiftung.

6 REFERENCES

[1] Tucher, N., Höhn, O., Murthy, J.N., *et al.*: 'Energy yield analysis of textured perovskite silicon tandem solar cells and modules', *Optics Express*, 2019, **27**, (20), A1419

[2] Sahli, F., Werner, J., Kamino, B.A., *et al.*: 'Fully textured monolithic perovskite/silicon tandem solar cells with 25.2% power conversion efficiency', *Nat Mater*, 2018, **17**, (9), pp. 820–826

[3] Schulze, P.S.C., Wienands, K., Bett, A.J., *et al.*: 'Perovskite Hybrid Evaporation/ Spin Coating Method: From Band Gap Tuning to Thin Film Deposition on Textures', *Thin solid films*, 2020, **704**, p. 137970

[4] Kamino, B.A., Paviet-Salomon, B., Moon, S.-J., *et al.*: 'Low-Temperature Screen-Printed Metallization for the Scale-Up of Two-Terminal Perovskite–Silicon Tandems', *ACS Applied Energy Materials*, 2019, **2**, (5), pp. 3815–3821

[5] Schulze, P.S.C., Bett, A.J., Bivour, M., *et al.*: '25.1% High‐Efficient Monolithic Perovskite Silicon Tandem Solar Cell with a High Band Gap Perovskite Absorber', *Solar RRL*, 2020, **4**, (7), p. 2000152

[6] Schubert, M.C., Mundt, L.E., Walter, D., Fell, A., Glunz, S.W.: 'Spatially Resolved Performance Analysis for Perovskite Solar Cells', *Adv. Energy Mater.*, 2020, p. 1904001

[7] Mundt, L.E., Heinz, F.D., Albrecht, S., *et al.*: 'Nondestructive Probing of Perovskite Silicon Tandem Solar Cells Using Multiwavelength Photoluminescence Mapping', *IEEE Journal of Photovoltaics*, 2017, **7**, (4), pp. 1081–1086

[8] Green, M., Dunlop, E., Hohl‐Ebinger, J., Yoshita, M., Kopidakis, N., Hao, X.: 'Solar cell efficiency tables (version 57)', *Prog Photovoltaics*, 2021, **29**, (1), pp. 3–15